METAL STRUCTURES CONFERENCE 1985

Performance of Structures

63
7
87

需要全本请访问 www.ertongbook.com

METAL STRUCTURES CONFERENCE 1985
'Performance of Structures'

MELBOURNE
23-24 MAY 1985
PREPRINTS OF PAPERS

Organised by:
The National Committee on Structural Engineering
of
The Institution of Engineers, Australia

PREFACE

The seventh Metal Structures Conference was organised by the National Committee on Structures of The Institution of Engineers, Australia and held at Monash University, Victoria.

The papers presented at this Conference have been grouped under six subject headings:

Dynamics, Strength of Members, Performance and Design, Bins, Numerical Methods and Reliability and Codes.

The papers reflect the current interests of engineers dealing with metal structures.

The organising committee wishes to thank all those who submitted papers for presentation at the Conference. Participants are urged to study those papers of interest prior to the Conference because authors will merely review their topics so as to allow maximum time for discussion.

The Organising Committee extends a very warm welcome to all participants and hopes that each will contribute to the exchange of ideas and therefore to the success of this Conference.

PAPERS

Stress Wave Effects in Steel Structures Subjected to Impact Loading ..... *S.H. Masood* . 1

Dynamic Analyses of Frames with Semi-Rigid Joints ..... *R. Kohoutek* 7

Axisymmetric Vibration of Annular Plates Using Receptances ..... *R.P. Brodzinski* 11

Static and Dynamic Analysis of Beams with a Single Discontinuity in Section ..... *R.P. Brodzinski and B.J. Stone* 15

Structural Damping in Bolted Beam Column Connections *A.K. Aggarwal and R.C. Coates* 20

The Strength of Long Length I-Section Columns Fabricated from Slender Plates ..... *A.J. Davids and G.J. Hancock* 26

Strength Tests of Cold Formed Square Hollow Section Columns ..... *P.W. Key and G.J. Hancock* 32

Stability and Design of Frames with Flexible Connections ..... *P. Grundy* 37

Double Diagonal Cross Bracing in Buildings ..... *S. Kitipornchai and D.L. Finch* 42

Ultimate Strength of Axially Compressed Stiffened Plates Containing Openings ..... *N.E. Shanmugam, P. Paramasivam and S.L. Lee* 48

Performance of a Steel Framed Kit House Tested for 63 m/s Cyclonic Winds ..... *G.F. Reardon and G.N. Boughton* 53

Inelastic Rotation Capacity of I-Sections for Portal Frame Design ..... *L.C. Schmidt and D.S. Mansell* 58

Tests on Tension Flange Braced Universal Beams ..... *S.N. Rao* 63

Design Testing and Operation of a Prototype Rotary Parking Machine ..... *P.J. Connolly and B.A. Vivian* 68

Behaviour of Liquid Storage Tanks Under Seismic Excitation ..... *R.K. Gupta, G.L. Hutchinson and A.C. Singhal* 73

The Performance of Buried Pipelines Subject to Ground Motion ..... *A.C. Singhal, G.L. Hutchinson and M.P. Chung* 82

Welded Steel Bins — An Introduction to AWRA Technical Note 14 ..... *B.E. Gorenc and I.W. McGeachie* 87

Buckling Behaviour of a Full-Scale Tank Under Internal and External Pressure ..... *M.J. Blackler and P. Ansourian* 92

Second-Order Analysis at Lap Joints of Cylindrical Silos and Tanks ..... *C.Y. Huang and P. Ansourian* 98

Elastic Buckling of Stiffened Ringbeams for Large Elevated Bins ..... *J.M. Rotter and P.T. Jumikis* 104

Buckling of Ground-Supported Cylindrical Steel Bins Under Vertical Compressive Wall Loads ..... *J.M. Rotter* 112

Computer Analysis of Steel Structures ..... *P.J. Stute, J.A. Tomas and S.M. Tinder* 128

A Finite Panel Method for Combined Plate Bending — Plane Stress Problems ..... *B.W. Golley and J. Petrolito* 133

Experimental and Analytical Study on Eccentrically Loaded Base Plates ..... *D.P. Thambiratnam, P. Paramasivam and N. Krishnamurthy* 138

Optimization of Cable Structures ..... *C.M. Wang and V. Thevendran* 143

Fatigue Strength of Beams at Cover Plate Terminations ..... *P. Grundy and S. Teh* 148

Influence of Load and Strength Correlation on the Performance of Metal Structures ..... *D.M. Frangopol* 154

Calibration of the Proposed Limit States Design Rules for Steel Beams and Columns ..... *L. Pham, R.Q. Bridge and M.A. Bradford* 160

Reliability Analysis of Bolted Connections for Structural Steelwork ..... *L. Pham and T.J. Hogan* 166

Survey of Research Needs for Metal Structures ..... *L. Pham and D.S. Mansell* 172

Metal Structures Conference,
1985, Melbourne, 23-24 May

Stress Wave Effects in Steel Structures Subjected to Impact Loading

S.H. MASOOD
Lecturer in Mechanical Engineering, University of Technology, Papua New Guinea

SUMMARY In many situations, the performance of steel structures is greatly affected by the presence of high intensity stress waves generated by transient loading. Attenuation of these waves is necessary for safe operation of structures. Elastomeric inserts have been used as a wave trap to alleviate the undesirable effects of stress waves. The paper presents an experimental analysis of the effects of stress waves through steel/elastomer interfaces in a simulated structural system and highlights the factors responsible for optimum design of elastomeric components. In particular, the modulus of rubber under impact conditions is investigated and a correlation between the dynamic behaviour of elastomer and the plastic behaviour of metals provides guidelines for selection of rubber components to achieve maximum attenuation of stress waves.

1 INTRODUCTION

The study of stress wave propagation in solids has been a matter of interest to researchers for a long time in view of problems involving high speed deformation processes as well as high impact destruction processes. High speed cutting, forging, pile driving, blast loading and failure in steel structure due to shocks are but few of many problems that call for a proper understanding of the phenomenon of stress waves and an appropriate design of systems involving these effects. Though the classical theories of elastic stress waves have been available for over a hundred years now, it is only in the last few decades that attempts have been made to apply these theories in understanding practical problems. However, the theories have not been readily applicable to design situations because solutions of three-dimensional stress wave equation for a real problem become mathematically intractable and those of one-dimensional equation are physically inconformable to the actual situation.

It is considered that the stress waves may lead to premature failure of mechanical components in steel structures by localised plastic flow or fatigue or fracture depending upon the mode of loading. Elastomers have been used in the wave path to attenuate these undesirable effects of stress waves. Commercial components, such as flexible coupling, anti-vibration mountings, bushes and belts are available using an elastomer and they have been applied more or less successfully in many industrial and structural situations. However the design of such components is usually carried out without involving any quantitative analysis of the effects of stress waves because sufficient information, both theoretical and experimental, is not available on which design decisions could be based.

In the design of elastomeric components used in structural systems, the modulus or stiffness of rubber is one of the major factors to be considered as its value depends considerably on the operating conditions. Extensive data are available for mechanical properties of rubber under static condition. The dynamic properties which are usually interpreted as the properties of rubber when subjected to cyclic deformation, are important in a large number of engineering applications and are generally more useful in the design of rubber springs and suspensions than the results of simpler static tests. Several test methods have been developed for dynamic properties involving either free vibration or forced vibration of the test piece (Brown, 1979). For the generation of engineering design data, forced vibration methods are generally considered to be the most useful. Wave propagation is one of these methods in which the dynamic modulus of rubber can be deduced from the velocity and attenuation of waves passing through it. A major limitation of the various systems developed so far involving wave propagation technique is that the specimen is subjected to sinusoidal excitation with frequency levels only upto 200 Hz (Payne and Scott, 1960). In many engineering structures, such as the mine hoisting system in a mining shaft, the components are subjected to impact loads, generating impact pulse of very high magnitude (of the order of half the yield strength of steel). For design of elastomeric components in such cases, the properties under transient conditions and particularly the modulus under impact loading conditions must be known. No such data appear to be available. Also the factors affecting the value of this modulus under such conditions do not appear to have been investigated.

This paper presents an investigation of the effects of stress waves through steel/elastomer interfaces in structures subjected to impact loads and highlights the major factors responsible for optimum design of elastomeric components. A specially designed apparatus is used to analyse the propagation of high impact stress waves in long steel bars through an elastomer inserted in a pair of connecting links. Preliminary experimental results obtained with this apparatus have highlighted the significance of high strain rates associated with stress waves, (Krok and Masood, 1979). The effect of preload, hardness and thickness of rubber specimens on the attenuation of stresses and strain rates have also been studied previously, (Masood and Krok, 1983). The present study is aimed at investigating the effect of strain rates on the impact modulus of elastomer under stress wave conditions. The study demonstrates an experimental technique to analyse the wave propagation in a structural system and lays down criteria of selection of modulus of rubber to achieve maximum attenuation of waves under impact loading conditions. As rubber is considered to be virtually incompressible, its dynamic behaviour is compared with the dynamic response of metal speci-

需要全本请访问 www.ertongbook.com

mens in plastic state under identical loading conditions in the apparatus. An interesting correlation is observed between the behaviour of rubber and lead and this fact is used to establish suitable guidelines for design of rubber components under transient loading conditions.

2 STRESS WAVE BEHAVIOUR

The simple one-dimensional theory of longitudinal wave propagation in linearly elastic bar predicts non-dispersive propagation of infinitesimal strain waves along the bar at a wave velocity $C_o = (E/\rho)$ and a relationship between the longitudinal stress σ and longitudinal particle velocity v, given by $\sigma = \rho C_o v$. In these expressions, ρ is the density and E the Young's Modulus of the bar material. The impedance Z of a component to propagation of stress waves is given by $Z = A\rho C_o$ where A is the cross-section area, (Johnson, 1972).

In considering the rubber inserts, since conditions will vary radially, it is more convenient to make the same assumption of elastic non-dispersive behaviour and express the relationship in terms of average axial quantities. With a knowledge of these quantities, the problem of propagation and attenuation of longitudinal stress waves through cylindrical rubber specimens can be analysed.

When stress wave propagates through the same cross-section of steel and rubber, the reflection and transmission of waves at steel/rubber interface is controlled by the ratio of impedances of the two materials, which in turn depends upon the density and the elastic modulus of each material. For steel, the Young's Modulus is a constant and within the elastic limit, the variation in density is negligible. Since rubber is virtually incompressible, the variation in its density may also be assumed to be negligibly small. This leaves the elastic modulus of rubber to be a major variable, which would control the reflection and transmission at the interface and hence would affect the magnitude of attenuation. In situation like impact loading, for which conventional test methods are not available, the value of elastic modulus of rubber, as derived from wave reflection and transmission, would be considered to be adequate for design of elastomeric components.

3 THE APPARATUS AND TEST PROCEDURE

The stress wave apparatus, shown schematically in Figure 1, consists of two vertical steel bars (approximately 18 mm diameter by 2500 mm long) each fitted with a rectangular link through which the load is applied to and received from the specimen. The bars are supported in a vertical frame (not shown), the top of the upper bar being attached through a rubber bush while the bottom of the lower bar has provision for preloading and for the initiation of stress waves by impact loading.

Preload is applied by an adjusting nut on the lower bar compressing conical washers against a reaction plate on the frame while the stress wave is initiated by dropping a mass onto a collar carried by the bottom end of the bar. With this arrangement the rubber specimen is loaded in compression which is necessary in this mode of operation and the long measuring bars are loaded in tension to maintain stability. The cylindrical rubber specimens used in the apparatus are bonded to thin steel end plates and have the same diameter as that of the measuring bars.

A dual beam storage cathode ray oscilloscope is used in single sweep mode with a standard time base to record the signals of the stress pulses from the strain gauges on the lower and upper measuring bars. A separate strain gauge on the lower bar is used to trigger the single sweep operation. The height of the recorded signal is a measure of the maximum strain in the bar while its slope is a measure of rate of loading or strain rate in the bar.

The stress wave apparatus represents a typical example of a steel structural system in which high impact propagating stress waves are involved and the effect of introduction of impedance mismatch is studied by observing the dynamic response of the steel members including the complex shaped rectangular links.

Elastomeric specimens of different shape factor can be used in the apparatus. A steel specimen is used for calibration purpose and for comparison of results. When steel specimen is used, the only impedance effect is due to the geometry of the rectangular links. This impedance change has no appreciable effect on the reduction of stress magnitude in steel bars but has a significant effect on the attenuation of strain rate.

When rubber specimens are used in the apparatus, both the rubber material and the geometry of the links cause the impedance changes. While the impedance due to geometry is a constant, the impedance due to rubber is influenced by the shape factor of rubber specimen as well as by the applied preload. The shape factor of a rubber component is defined as the ratio of the cross-section area normal to the

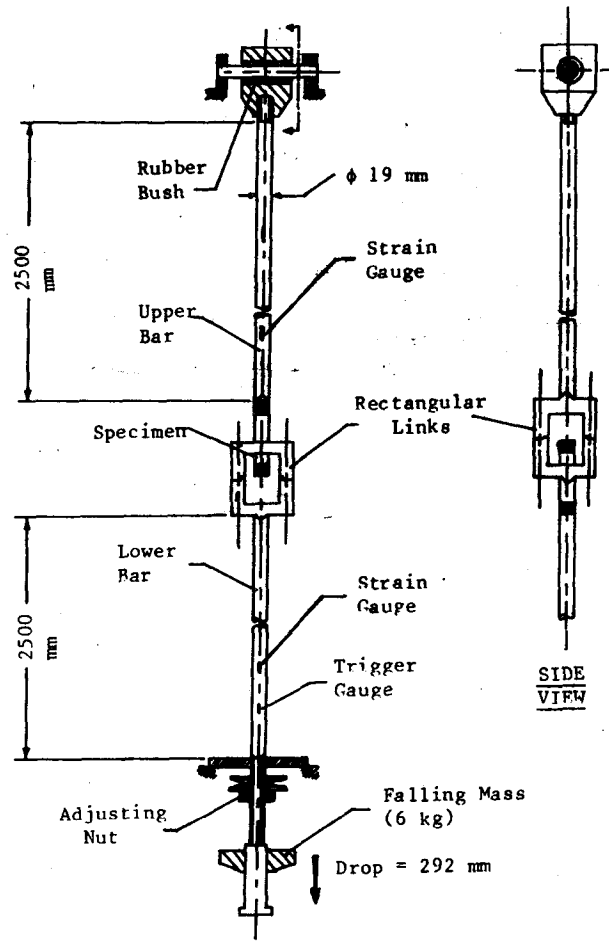


Figure 1 The Stress Wave Apparatus

the direction of the stress wave to the free surface area parallel to the direction of the wave. This relationship is important in the design of rubber components used to attenuate the consequences of impact loading.

The experimental test procedure basically consists of determining the magnitude of the reflected stress in the lower bar for each test of rubber specimen and then determining the dynamic impedance, the wave velocity and the impact modulus by using one-dimensional stress wave theory. As the magnitude of reflected stress depends upon the magnitude of incident impact stress, the rubber hardness, the shape factor and the applied preload, the value of impact modulus would change with variation in any of these parameters. In the computation of the modulus of rubber, the impedance change due to geometry of the rectangular links is considered and the apparatus is represented as a geometric model consisting of a series of co-axial cylinders of appropriate acoustic impedance determined by a separate analysis, (Masood, 1983). Results have been obtained with cylindrical rubber specimens of same diameter (19 mm) but of different thickness (2.3 to 13 mm) and hardnesses. Maximum range of results were obtained for the hardest rubber specimens as softer and thicker specimens induce buckling problems. The curves of impact modulus (E_R) variation with strain rate at various preloads (P) and shape factors (S) for the hardest rubber specimens are shown in Figures 2 and 3 while those for medium hard specimens are shown in Figures 4 and 5. The results for soft specimens are plotted in Figure 6 only for zero preload.

4 DISCUSSION OF RESULTS

The curves plotted in Figures 2 to 6 give a general trend of the behaviour of dynamic stiffness of rubber used in specific conditions of the stress wave apparatus. For each rubber material, having a specific shape factor and a hardness, the impact modulus is very sensitive to the strain rate and preload variation. All the curves shown in Figures 2 and 3 indicate that the modulus increases with strain rate as well as with preload. Comparing the curves in these figures, it is observed that the magnitudes of moduli are very high for rubber specimens of highest shape factor, S = 2.06, as compared to those of smaller shape factors. For specimens of similar shape factors, the moduli of the harder rubber specimens are larger than those of soft rubber specimens. Curves in Figure 2 show that rubber specimens of very high shape factor or very small axial thickness would have very high stiffness even at low strain rate and small preload and therefore rubber components of such characteristic would not be suitable for stress attenuation or strain rate attenuation. Comparing the Figures 2 and 3, it is noted that the components with smaller shape factor and higher preload would have almost the same dynamic effect on the rubber stiffness as the components with larger shape factor and smaller preload. Figures 4,5 and 6 show that the value of impact modulus is low for softer rubber specimens but increases with an increase of preload and an increase of shape factor.

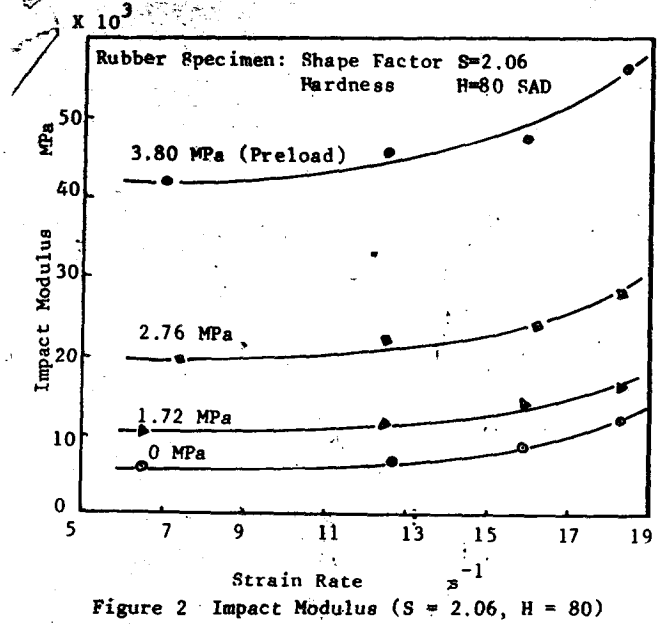


Figure 2 Impact Modulus (S = 2.06, H = 80)

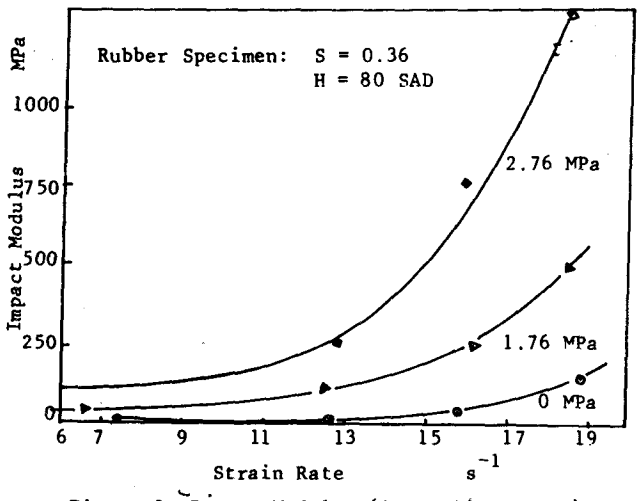


Figure 3 Impact Modulus (S = 0.36, H = 80)

The curves shown in Figures 2 to 6 provide a general quantitative idea of the magnitudes of the approximate values of impact modulus of rubber under various conditions of shape factor, preload and strain rate used in a typical structural system. These are useful inthe selection of elastomeric components designed for attenuation of stress waves. If an appropriate value of the effective modulus of rubber in a particular situation is known, it can be used to determine the effective impedance of rubber

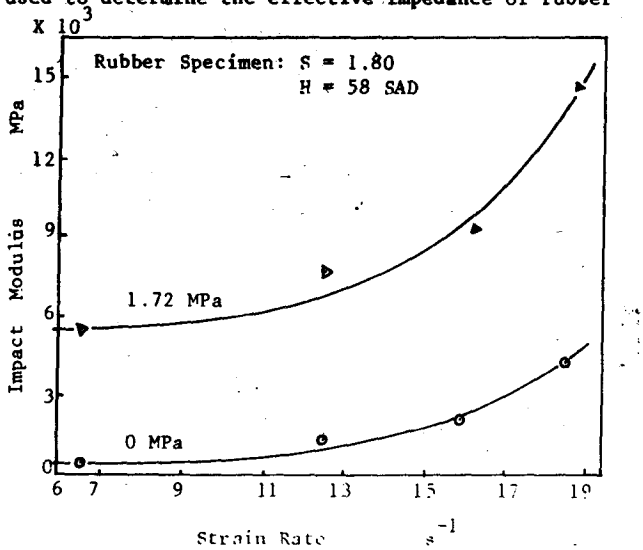


Figure 4 Impact Modulus (S = 1.80, H = 58)

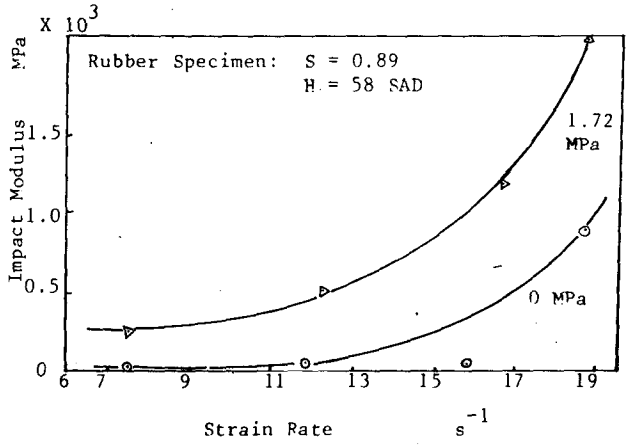


Figure 5 Impact Modulus (S = 0.89, H = 58)

and the stress attenuation factor, which would provide a suitable criterion of selection of rubber components.

5 COMPARISON WITH BEHAVIOUR OF METALS

The design and versatility of the stress wave apparatus has made it possible to compare the dynamic behaviour of elastomers and metals under stress wave conditions and thereby deduce some useful design information for rubber components used in structures. The stress-strain behaviour of rubber differs widely from that of metals. While rubber within the elastic limit has a non-linear stress-strain characteristics and is virtually incompressible with large recoverable deformation capability under small forces, metals have a linear and compressible behaviour and exhibit small deformation under large applied forces. In the plastic state, however, metals are essentially incompressible and show a large permanent deformation for a small increase in force. Thus there appears to be some similarities between the plastic behaviour of metals and the elastic behaviour of elastomers. In the study of the plastic flow of metals, the well known slip-line field theory is based on the assumption of a rigid plastic material and gives acceptable results in the evaluation of loads and velocities in certain metal working operations (Hill, 1950). Among common engineering metals, pure lead fulfils the requirements of the slip-line theory and can thus be chosen as an ideal meterial for theoretical and experimental investigation of its incompressible behaviour in plastic state at a room temperature.

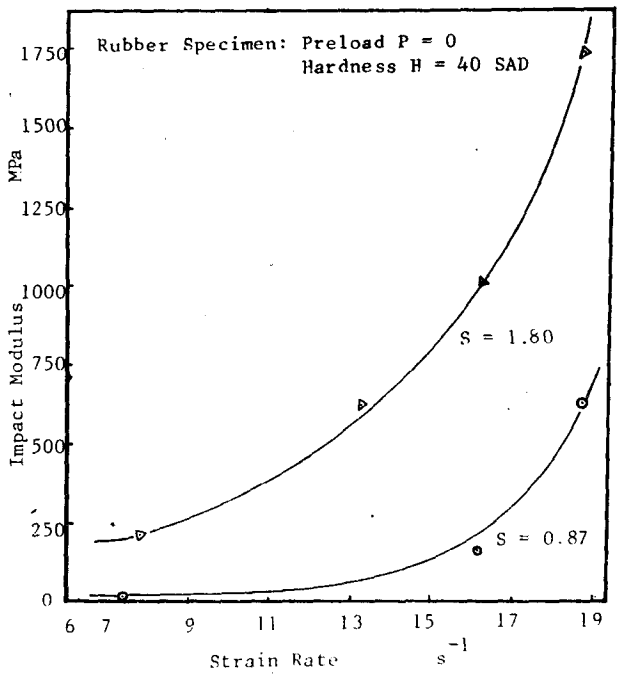


Figure 6 Impact Modulus (P = 0, H = 40)

The experimental tests of rubber specimens on the stress wave apparatus have shown that the dependence of rubber modulus on shape factor, preload and hardness is most critical. The variation of impact modulus with thickness for hardest rubber specimens is shown in Figure 7 for a given value of impact load but for three different values of applied preload. At the instant of impact loading, the effective impedance of rubber changes suddenly. As rubber is incompressible, there is virtually no change in density, and therefore the change in impedance is due to the change in impact modulus of rubber. Similar results can be expected for modulus of lead under plastic deformation which is incompressible.

Experimental tests were performed with lead specimens of different thicknesses (3 to 15 mm) and constant diameter (19 mm) on the stress wave apparatus. As in the case of rubber, the lead specimens were also bonded to steel ends to achieve similar end effects. No preload was necessary since it does not affect the molecular structure of lead. At the instant of impact loading, the lead undergoes plastic deformation, attains incompressibility and its effective impedance decreases sharply. This impedance change is attributed to the change in the dynamic modulus of lead. An appreciable amount of reflected stress wave is observed in the lower bar. The variation of dynamic modulus of lead (E_L), calculated from stress wave theory, with the thickness is shown in Figure 8 for two values of impact stress (ρ_I).

Comparison of Figures 7 and 8 indicate that under identical stress wave test conditions, rubber and lead exhibit similar patterns of dynamic characteristics. For lead specimens, like rubber, the interface effect and not the internal structure of material appears to be the main controlling factor in the reflection and transmission of stress waves. It appears that the common factor of incompressibility is very significant in making the two materials comparable under dynamic loading. While a complete theoretical analysis of metals under dynamic situation is not readily available, the slip-line theory offers a convenient method of correlation between the static and dynamic behaviour of lead.

Figure 9 shows the variation of apparent modulus of lead with thickness, which has been obtained by considering the average pressure required for the quasi-static compression of lead blocks between two rough plates using the slip-line theory. This curve, which has the same form as the experimental curve of Figure 8, provides a more realistic appreciation of modulus of lead in terms of deformation at a constant stress. This correlation between the static and dynamic behaviour of lead and the common trend between the dynamic behaviour of lead and rubber can be used to provide initial solutions to the design of rubber blocks under impact conditions.

6 DESIGN CONSIDERATIONS

The results of the experimental tests on the stress wave apparatus provide a reasonable guidance for the selection of impact modulus and shape factor of

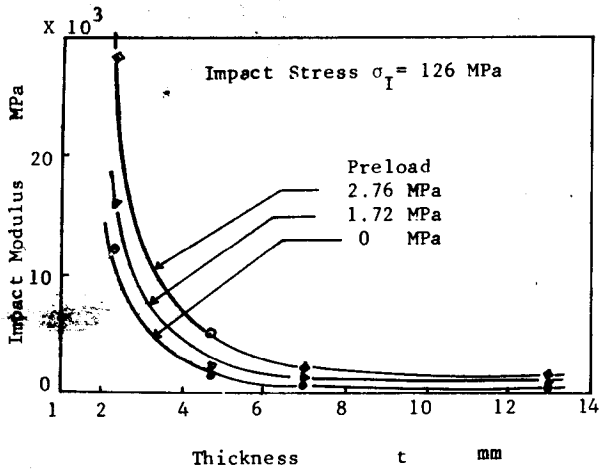


Figure 7 Variation of Modulus with thickness

rubber for specific situations. For maximum attenuation of stress waves in steel structures, the impedance of the damping material should be as low as possible. Since rubber is an incompressible material its density remains constant, so the attenuation could be increased if rubber components are designed to have a low dynamic modulus. However, the choice of low modulus is limited by the size of the component and the magnitudes of applied preloads and strain rates. In structural systems, rubber is always subjected to certain preload, the applied dynamic stresses are normally fixed according to requirements, and the size of the rubber component is often decided by other factors. In such cases, the components should be designed such that an optimum shape factor is used. Such a shape factor would provide an optimum modulus for rubber under given loading conditions and would therefore ensure maximum attenuation of stress waves.

The variation in slope of the curve in Figure 7 indicates how far the values of modulus varies with thickness. The desirable point would be one where the slope of the curve is fairly small or near zero and remains so for a range of thicknesses. For specimens of thickness 8 mm and higher, the slope is nearly zero and fairly steady. The specimens in this range will ensure maximum reflection and minimum transmission of waves through the rubber thus providing maximum safety against stress wave effects.

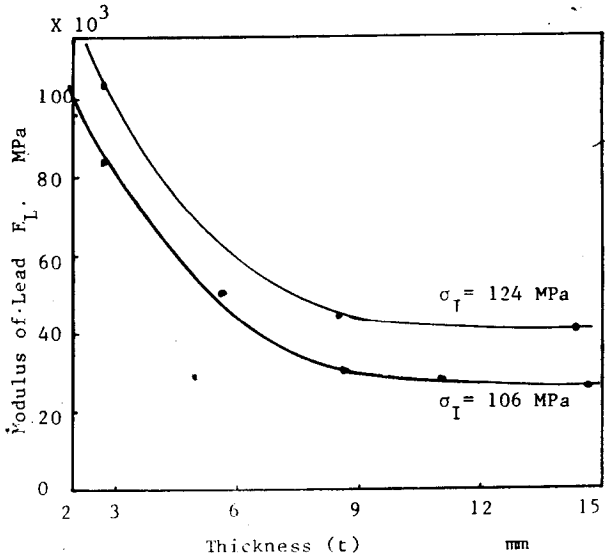


Figure 8 Impact Modulus of Lead

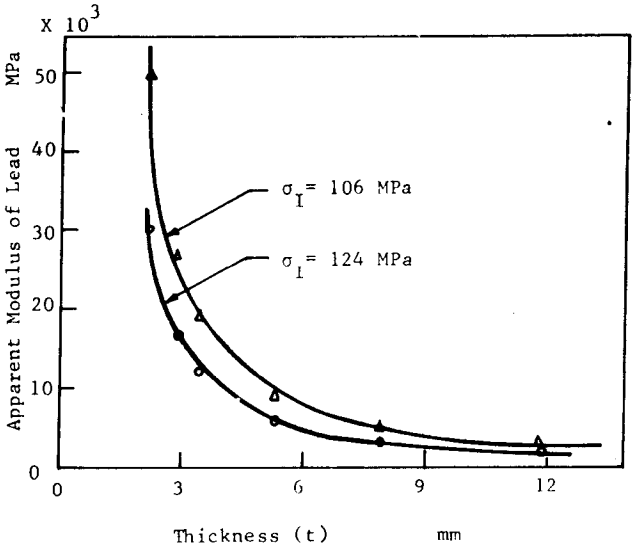


Figure 9 Apparent Modulus of Lead

However specimens of these sizes would not be able to bear high preload and high impacts and would be liable to buckling failure. The specimens in the range 2 to 4 mm will no doubt be more stable and capable of high loads but as the slope of the curves increases sharply in this range, they would not be able to provide sufficient attenuation. The specimens of optimum size appear to be in the range of 4 to 7 mm thickness. In this range the variation in slope with thickness is not very great, the magnitudes of effective modulus are small, and the specimens would be able to sustain reasonable amount of preload and impact stress. These specimens would provid optimum attenuation of stress waves and would be stable under given conditions of loading.

Results of lead specimens, shown in Figure 8, indicate that, like in rubber tests, the value of impact modulus of lead also increases asymptotically for very thin specimens but remains fairly steady for thicker specimens. The variation of the slope of the curve is identical to that of the curves for rubber specimens, and the range of 6 mm to 9 mm appear to be the optimum range. This same range can also be seen to be the optimum thickness range by reference to Figure 9, which gives the theoretical results of slip-line field analysis.

The tests on stress wave apparatus have thus provided a qualitative and a quantitative approach to the design of rubber components under impact loading conditions. Curves of slip-line field theory - apparent modulus vs thickness - provide the criterion of selection of an optimum thickness or an optimum shape factor for the component in order to attain a low value of modulus. This is a qualitative criterion. The curves of rubber tests - impact modulus vs thickness provide the guidelines for selection of an optimum rubber modulus for a chosen thickness or shape factor for a specific applied impact load and a simultaneous preload. This is the quantitative criterion.

7 CONCLUSIONS

An experimental study of the dynamic response of a structural system involving high impact stress wave has been made. Stress wave theory offers a convenient technique of deriving the impact modulus of rubber components used to alleviate the adverse effects of stress waves in steel structures. The modulus of rubber is found to be greatly affected by the variation in applied strain rate, preload,

hardness and shape factor. A proper selection of impact modulus of elastomer based on these factors is critical in order to improve the performance of steel structures in transient conditions. A correlation between the dynamic behaviour of rubber and the plastic behaviour of lead is observed under stress wave conditions. This has been used to establish quantitative and qualitative criteria for optimum design of rubber components used under such conditions.

8 REFERENCES

BROWN, R.P. (1979). Physical Testing of Rubber. Applied Sc. Pub. Ltd., London.

HILL, R. (1950). The Mathematical Theory of Plasticity. The Clarendon Press, Oxford.

JOHNSON, W. (1972). Impact Strength of Materials. Edward Arnold, London.

KROK, T.V. and MASOOD, S.H. (1979). The Attenuation of Stress Waves by Elastomers. Int. Conf. on Mining Machinery, I.E. Aust., Pub. No. 79/5, pp 575-80.

MASOOD, S.H. (1983). Attenuation and Propagation of Axisymmetric Stress Waves Through Rubber Cylinders. Ph.D. Thesis, University of Queensland.

MASOOD, S.H. and KROK, T.V. (1983). An Experimental Study of Stress Wave Attenuation. Mech. Eng. Trans., I.E. Aust., Vol. ME8, No. 1, June 1983, pp 39-45.

Metal Structures Conference,
1985, Melbourne, 23-24 May

Dynamic Analyses of Frames with Semi-Rigid Joints

R. KOHOUTEK
Lecturer, University of Wollongong

SUMMARY A method is presented for analyses of frames with semi-rigid joints. The dynamic deformation method used for analysis is suitable for free or forced vibrations. The method incorporates all influences such as semi-rigidity, axial force, rotary inertia and shear force into one expression with improved numerical stability desirable for computer modelling.

1 INTRODUCTION

The underlying common assumption for the analysis of frames is complete rigidity of the joints. The shortcomings of this assumption have been recognised for some time ([2,3] Baker 1930). During the last decade renewed interest in the topic is shown by the number of published papers, extending the original static, linear analysis into the plastic range as well as taking some dynamic behaviour into account. Also the original investigation dealing with steel member connection has been expanded into composite structures and reinforced concrete. The majority of research papers consider that the loads produce some plastic deformations. Furthermore, quasi-static load is favoured, typically of several herts; possibly because of the difficulty of inducing higher frequencies under complete control. In this analysis only small deformations are assumed and the analysis shown here follows Firt [1], which assumes completely rigid "core" of a joint and semi-rigid connection (a semi-rigid hinge) of a bar to the core.

2 PROBLEM FORMULATION

Consider a bar of the constant flexural stiffness EI and the constant mass m connected semi-rigidly to the infinitely rigid cores

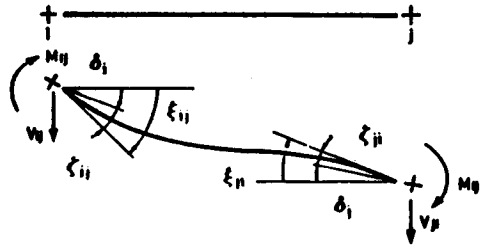


Figure 1. Deformations and forces on a bar with semi-rigid joints.

For the purpose of our analysis we assume that a rather complicated relationship between the forces and deformations, which occurs at the joints, can be approximated by a single functional relationship which in general is

$$M_{ij} = \frac{EI}{l} \varphi_{ij}(N, \xi_{ij}, \ldots) \quad \text{and}$$
$$M_{ji} = \frac{EI}{l} \varphi_{ji}(N, \xi_{ji}, \ldots). \tag{1}$$

The functions φ depend on several parameters (not completely specified here) such as an axial force N, and angle of rotation. No loss of generality will occur in the following procedure which considers these two parameters. The φ functions can be expanded by a Taylor series about the origin to give

$$\varphi_{ij} = C_{1,ij} + C_{2,ij}\varepsilon^2 + C_{3,ij}\varepsilon^4 + C_{4,ij}\xi_{ij} + C_{5,ij}\xi_{ij}^2 + \ldots$$
$$\varphi_{ji} = C_{1,ji} + C_{2,ji}\varepsilon^2 + C_{3,ji}\varepsilon^4 + C_{4,ji}\xi_{ji} + C_{5,ji}\xi_{ji}^2 + \ldots \tag{2}$$

where C_i are constants and ε is a parameter reflecting the influence of an axial force. The above step is justified only for small deformations, which is sufficient to allow the natural frequencies to be investigated. However, it does not allow the amplitudes of deformations for undamped vibrations to be established and only shapes (eigenfunctions) can be calculated. For the investigations of vibrations in the elastic range presented here, the claim that linear relationship exists between moment and rotation made by Firt [1], and Faulkner [2] seems justified.

3 LINEAR ANALYSIS

For this case equation (1) will be simplified to

$$M_{ij} = -\frac{EI}{l}\gamma_{ij}\zeta_{ij} \quad \text{and}$$
$$M_{ji} = -\frac{EI}{l}\gamma_{ji}\zeta_{ji} \tag{3}$$

with the relationship between γ_{ij} and ζ_{ij} from Figure 1 being given by

$$\xi_{ij} = \delta_i + \zeta_{ij} \quad \text{and}$$
$$\xi_{ji} = \delta_j + \zeta_{ji}. \tag{4}$$

需要全本请访问 www.ertongbook.com

Hence, from (3) and (4),

$$\xi_{ij} = \delta_i - \frac{lM_{ij}}{EI\,\gamma_{ij}} \quad \text{and}$$

$$\xi_{ji} = \delta_i - \frac{lM_{ji}}{EI\,\gamma_{ji}} \tag{5}$$

where γ_{ij} and γ_{ji} are constants representing the semi-rigidity of a joint for the particular bar/joint connection.
The common view, and the one adopted here, is that only the moment is primarily affected, while the shear force is carried through the joint. Equation (5) fully describes this class of a semi-rigid joint.
The relationships between bending moments and the shear forces in the deformation method are given in Table 1 (details are given in Kohoutek [9]).

TABLE 1
Forces due to unit deformations Clamped – clamped beam

	$\xi_i = 1$	$w_i = 1$	$\xi_j = 1$	$w_j = 1$
M_{ij}	$\frac{EI}{l} F_2$	$\frac{EI}{l^2} F_4$	$\frac{EI}{l} F_1$	$\frac{EI}{l^2} F_3$
V_{ij}	$\frac{EI}{l^2} F_4$	$\frac{EI}{l^3} F_6$	$\frac{EI}{l^2} F_3$	$\frac{EI}{l^3} F_5$
M_{ji}	$\frac{EI}{l} F_1$	$\frac{EI}{l^2} F_3$	$\frac{EI}{l} F_2$	$\frac{EI}{l^2} F_4$
V_{ji}	$\frac{EI}{l^2} F_3$	$\frac{EI}{l^3} F_5$	$\frac{EI}{l^2} F_4$	$\frac{EI}{l^3} F_6$

These expressions can be rewritten in a more suitable form for further manipulation and are listed below.

$$M_{ij} = \frac{EI}{l}\left(F_2 \xi_{ij} + F_1 \xi_{ji} - F_4 \frac{w_{ij}}{l} - F_3 \frac{w_{ji}}{l}\right)$$

$$M_{ji} = \frac{EI}{l}\left(F_1 \xi_{ij} + F_2 \xi_{ji} + F_3 \frac{w_{ij}}{l} + F_4 \frac{w_{ji}}{l}\right) \tag{6}$$

$$V_{ij} = \frac{EI}{l^2}\left(-F_4 \xi_{ij} + F_3 \xi_{ji} + F_6 \frac{w_{ij}}{l} + F_5 \frac{w_{ji}}{l}\right)$$

$$V_{ji} = \frac{EI}{l^2}\left(-F_3 \xi_{ij} + F_4 \xi_{ji} + F_5 \frac{w_{ij}}{l} + F_6 \frac{w_{ji}}{l}\right)$$

The equations (6) can be expressed in matrix notation as

$$\begin{bmatrix} \mathbf{M} \\ \mathbf{V} \end{bmatrix} = \mathbf{F} \begin{bmatrix} \xi \\ w \end{bmatrix} \tag{7}$$

Substitution of equation (5) into equation (7) yields

$$\begin{bmatrix} \mathbf{M} \\ \mathbf{V} \end{bmatrix} = \mathbf{F} \begin{bmatrix} \delta \\ w \end{bmatrix} = \mathbf{F} \begin{bmatrix} \xi + lM/\gamma EI \\ w \end{bmatrix}$$

and

$$\begin{bmatrix} \mathbf{M} \\ \mathbf{V} \end{bmatrix} = \mathbf{F} \begin{bmatrix} lM/\gamma EI \\ 0 \end{bmatrix} + \mathbf{F} \begin{bmatrix} \xi \\ w \end{bmatrix}$$

Defining a new matrix $\mathbf{F}_1^{-1}$ by $\mathbf{F}_1 = \mathbf{I} - \mathbf{F}$ (defined in Appendix 2) leads to

$$\mathbf{F}_1 \begin{bmatrix} \mathbf{M} \\ \mathbf{V} \end{bmatrix} = \mathbf{F} \begin{bmatrix} \xi \\ w \end{bmatrix}$$

$$\begin{bmatrix} \mathbf{M} \\ \mathbf{V} \end{bmatrix} = \mathbf{F}_1^{-1}\mathbf{F} \begin{bmatrix} \xi \\ w \end{bmatrix} = \Phi \begin{bmatrix} \delta \\ w \end{bmatrix} \tag{8}$$

The matrix $\mathbf{F}_1^{-1}$ enables a new definition of frequency functions Φ_n, n = 1,6 which incorporates the semi-rigidity of the individual connections. The detailed derivation is given in Appendix 1, with the new frequency functions listed below. Since the limit cases of semi-rigidity are hinge and complete fixity, only six frequency functions are required to cover all basic support conditions.

$$\Phi_1(ij) = \gamma_{ij}\, D^{-1}\, F_1\, \gamma_{ji}$$

$$\Phi_2(ij) = \gamma_{ij}\, D^{-1}\,(F_2\, \gamma_{ji} - F_2^2 + F_1^2)$$

$$\Phi_3(ij) = \gamma_{ij}\, D^{-1}\,(-F_3\, \gamma_{ji} + F_2 F_3 + F_1 F_4)$$

$$\Phi_4(ij) = \gamma_{ij}\, D^{-1}\,(-F_4\, \gamma_{ji} + F_2 F_4 + F_1 F_3) \tag{9}$$

$$\Phi_5(ij) = F_5 + D^{-1}(-F_1 F_4^2 + F_3 F_4 (\gamma_{ji} + \gamma_{ij} - 2F_2) - F_1 F_3^2)$$

$$\Phi_6(ij) = F_6 + D^{-1}(F_4^2 (\gamma_{ij} - F_2) - 2F_1 F_3 F_4 + F_3^2 (\gamma_{ji} - F_2))$$

where

$$D = \gamma_{ji}\, \gamma_{ij} - F_2 (\gamma_{ji} + \gamma_{ij}) + F_2^2 - F_1^2.$$

Frequency functions in the other direction (ji) on a bar are simply created from (9) by the interchange of idexes *ij* and *ji*. The arguments of the frequency function F_n for the rigid joint are ommited for clarity.

Different types of frequency functions are possible:

(*i*) $F(\lambda)$ when only flexural deformation is considered and

(*ii*) $F(a,d)$ when the effects of axial force, shear deformations, rotary inertia and some forms of damping, are included either individually or in some combination. The algorithms for natural frequencies, forced vibrations [9] and dynamic stability [7], are maintained but the computational effort is substantially increased because of (9).

4 CONCLUSIONS

The boundary conditions play an important role in all dynamic analyses. The correct estimation of the boundary conditions significantly influences the determinations of: the static critical load (Sweet et al) [11], Segal and Barnuch [10]); natural frequencies (Firt [1], Faulkner [2], Kohoutek [4]); and dynamic stability (Kohoutek [6,7]).

Generalised boundary conditions such as those applying at a joint in the frame will have a major influence on *all the critical design parameters* above. The derivation of modified frequency functions for linear semi-rigid joints permits the dynamic deformation method to be used in the investigation of dynamic stability problems, as well as in static stability and natural frequencies, which are only special cases of dynamic stability.

Further research is needed to ascertain whether the linearity, the affect of a frequency on and the influence of an axial force should be incorporated into the analysis of a semi-rigid joint. The influence of an axial force was obviously present in Carlson's experiment and modified the boundary conditions (Kohoutek [6]).

The linear analysis is computationally difficult but feasible for some important structures.

5 ACKNOWLEDGEMENT

The work was conducted at the Department of Civil Engineering of the University of Melbourne with the aid of Writing-Up Award received from the University of Melbourne.

6 REFERENCES

[1] Firt, V. (1974).Stabilita a kmitani konstrukci s netuhymi spoji (Stability and Vibrations of Structures with Semi-rigid joints), Academia - Praha.

[2] Howlett,J.H. et al (1981).Joints in Structural Steelwork, Proceedings of the International Conference held at Teesside Polytechnic, Cleveland, 6-9 April 1981. Pentech Press.

[3] Jones, S.W., Kirby, P.A., and Hethercot, D.A. (1983).The Analysis of Frames with Semi-rigid Connections - A State of Art Report, Journal of Constructional Steel Research, V.3, #2.

[4] Kohoutek, R. (1980).Spring-hinged beam, Research Report RR/Struct/04/1980, University of Melbourne.

[5] Kohoutek, R. (1983).Computational improvements of the Dynamic Deformation Method, Computational Techniques and Application Conference, University of Sydney, August.

[6] Kohoutek, R. (1984).The Dynamic Instability of the Bar Under Tensile Periodic Force, Trans. of Canadian Society of Mechanical Engineers.

[7] Kohoutek, R. (1985). The Dynamic Stability of Frames by the Deformation Method, 19th Midwestern Mechanics Conference The Ohio State University, September 9-11.

[8] Kohoutek, R. (1985). Computational aspects of dynamic analysis of frames with semi-rigid joints, Computational Techniques and Application Conference, University of Melbourne August.

[9] Moore, P. J. et al. (1985).Analysis and Design of Foundation for Vibrations, Ch. 4 "Dynamic Analysis of Frames", A.A.Balkema.

[10] Segall, A. and Barnuch, M. (1980). A Nondestructive Dynamic Method for the Determination of the Critical Load of Elastic Columns, Experimental Mechanics-October, pp. 385-391.

[11] Sweet, A.L.,Genin, J. and Mlakar, P.F.(1977).Determination of Column-buckling Criteria Using Vibratory Data, Experimental Mechanics - August pp. 285-288.

[12] Tan, T. H. (1985). The Rigidity of Steel Connections PhD Thesis, University of Melbourne, in progress.

APPENDIX 1

Derivation of frequency functions for semi-rigid joints.

A general outline is given by equations (7) to (8) and this will not be repeated here. The problem is reduced to a definition of $\mathbf{F}_1$, and its inversion $\mathbf{F}_1^{-1}$ and an evaluation of a product $\mathbf{F}_1^{-1}\mathbf{F}_1$.

The matrix $\mathbf{F}_1 = \mathbf{I} - \mathbf{F}$ is, in full,

$$\mathbf{F}_1 = \begin{bmatrix} \mathbf{I} & \mathbf{0} \\ \mathbf{0} & \mathbf{I} \end{bmatrix} - \begin{bmatrix} \mathcal{F}_1 & \mathbf{0} \\ \mathcal{F}_2 & \mathbf{0} \end{bmatrix} = \begin{bmatrix} 1 - F_2/\gamma_{ij} & -F_1/\gamma_{ji} & 0 & 0 \\ -F_1/\gamma_{ij} & 1 - F_2/\gamma_{ji} & 0 & 0 \\ F_4/\gamma_{ij} & -F_3/\gamma_{ji} & 1 & 0 \\ F_3/\gamma_{ij} & -F_4/\gamma_{ji} & 0 & 1 \end{bmatrix}$$

which can be written as

$$\mathbf{F}_1 = \begin{bmatrix} \mathbf{I} - \mathcal{F}_1 & \mathbf{0} \\ -\mathcal{F}_2 & \mathbf{I} \end{bmatrix} \text{ with the inverse } \begin{bmatrix} \mathcal{P} & \mathcal{Q} \\ \mathcal{R} & \mathcal{S} \end{bmatrix} = \mathbf{F}_1^{-1}. \quad \text{(A 1.1)}$$

The identity matrix

$$\mathbf{I} = \mathbf{F}_1\mathbf{F}_1^{-1} = \begin{bmatrix} (\mathbf{I} - \mathcal{F}_1)\,\mathcal{P} = \mathbf{I} & (\mathbf{I} - \mathcal{F}_1)\,\mathcal{Q} = \mathbf{0} \\ -\mathcal{F}_2\mathcal{P} + \mathcal{R} = \mathbf{0} & -\mathcal{F}_2\mathcal{Q} + \mathcal{S} = \mathbf{I} \end{bmatrix} \quad \text{(A 1.2)}$$

implies the following relationships:

$$\mathcal{P} = (\mathbf{I} - \mathcal{F}_1)^{-1};$$
$$\mathcal{Q} = \mathbf{0};$$
$$\mathcal{R} = \mathcal{F}_2(\mathbf{I} - \mathcal{F}_1)^{-1}; \text{ and}$$
$$\mathcal{S} = \mathbf{I}.$$

Hence

$$\mathbf{F}_1^{-1} = \begin{bmatrix} (\mathbf{I} - \mathcal{S}_1)^{-1} & \mathbf{0} \\ \mathcal{S}_2(\mathbf{I} - \mathcal{S}_1)^{-1} & \mathbf{I} \end{bmatrix} \qquad \text{(A 1.3)}$$

The first submatrix of (A 1.3), in full, is

$$\mathcal{P} = (\mathbf{I} - \mathcal{S}_1)^{-1} = \begin{bmatrix} (\gamma_{ij} - F_2)/\gamma_{ij} & -F_1/\gamma_{ji} \\ -F_1/\gamma_{ij} & (\gamma_{ji} - F_2)/\gamma_{ji} \end{bmatrix}^{-1} =$$

$$= D_1^{-1} \begin{bmatrix} (\gamma_{ji} - F_2)/\gamma_{ji} & F_1/\gamma_{ji} \\ F_1/\gamma_{ij} & (\gamma_{ij} - F_2)/\gamma_{ij} \end{bmatrix} \qquad \text{(A 1.4)}$$

where

$$D_1 = (\gamma_{ij}\gamma_{ji} - F_2(\gamma_{ji} + \gamma_{ij}) + F_2^2 - F_1^2)/\gamma_{ij}\gamma_{ji}.$$

The second submatrix of (A 1.3) similarly gives

$$\mathcal{R} = \mathcal{S}_2(\mathbf{I} - \mathcal{S}_1)^{-1} = D^{-1} \begin{bmatrix} -F_4/\gamma_{ij} & F_3/\gamma_{ji} \\ -F_3/\gamma_{ij} & F_4/\gamma_{ji} \end{bmatrix}.$$

$$\begin{bmatrix} (\gamma_{ij} - F_2)\gamma_{ji} & F_1\gamma_{ij} \\ F_1\gamma_{ji} & (\gamma_{ij} - F_2)\gamma_{ji} \end{bmatrix} =$$

$$- D^{-1} \begin{bmatrix} -F_4(\gamma_{ji} - F_2) + F_3F_1 & F_3(\gamma_{ij} - F_2) - F_4F_1 \\ -F_3(\gamma_{ji} - F_2) + F_4F_1 & F_4(\gamma_{ij} - F_2) - F_3F_1 \end{bmatrix} \qquad \text{(A 1.5)}$$

The inverse $\mathbf{F}_1^{-1}$ defined by (A 1.3), using (A 1.4) and (A 1.5), is

$$D_1^{-1} \begin{bmatrix} (\gamma_{ji} - F_2)/\gamma_{ji} & F_1/\gamma_{ji} & 0 & 0 \\ F_1/\gamma_{ij} & (\gamma_{ij} - F_2)/\gamma_{ij} & 0 & 0 \\ -F_4(\gamma_{ji} - F_2) + F_3F_1 & F_3(\gamma_{ij} - F_2) - F_4F_1 & D_1 & 0 \\ -F_3(\gamma_{ji} - F_2) + F_4F_1 & F_4(\gamma_{ij} - F_2) - F_3F_1 & 0 & D_1 \end{bmatrix} \qquad \text{(A 1.6)}$$

The product $\mathbf{F}_1^{-1}\mathbf{F}$, with $\mathbf{F}_1^{-1}$ given by (A 1.6) and $\mathbf{F}$ from Table 1, gives modified frequency functions (Appendix 2) for semi-rigid joints described by (6). Here only the six functions are needed because limit cases cover both hinge and fixed connections. The frequency functions for clamped-clamped support conditions, considering only flexural deformations are given in Appendix 3.

APPENDIX 2

Frequency functions $\Phi_i(ij)$

The frequency functions F_i , i = 1,6 could be those of Appendix 3, if only flexural deformation is considered or F_i (a,d) of [7], if the influences such as shear deformations, rotary inertia and axial force are included.

$$\Phi_1(ij) = \gamma_{ij}\, D^{-1} F_1\, \gamma_{ji}$$

$$\Phi_2(ij) = \gamma_{ij}\, D^{-1} (F_2\, \gamma_{ji} - F_2^2 + F_1^2)$$

$$\Phi_3(ij) = \gamma_{ij}\, D^{-1} (-F_3\, \gamma_{ji} + F_2 F_3 + F_1 F_4)$$

$$\Phi_4(ij) = \gamma_{ij}\, D^{-1} (-F_4\, \gamma_{ji} + F_2 F_4 + F_1 F_3)$$

$$\Phi_5(ij) = F_5 + D^{-1}(-F_1 F_4^2 + F_3 F_4 (\gamma_{ji} + \gamma_{ij} - 2F_2) - F_1 F_3^2)$$

$$\Phi_6(ij) = F_6 + D^{-1}(F_4^2 (\gamma_{ij} - F_2) - 2F_1 F_3 F_4 + F_3^2 (\gamma_{ji} - F_2))$$

where

$$D = \gamma_{ji}\, \gamma_{ij} - F_2(\gamma_{ji} + \gamma_{ij}) + F_2^2 - F_1^2.$$

APPENDIX 3

Frequency functions $F_i(\lambda)$

The frequency functions for vibration without damping; only flexural deformations are considered. The first six frequency functions needed are shown here (clamped – clamped bar); for other basic support conditions: hinged – clamped, cantilever, and hinged – hinged refer to [7] or [9].

A parameter λ is calculated from

$$\lambda = l\, (m\omega^2/EI)^{0.25}$$

where l is a length of the beam, m is a mass per unit length, ω is a frequency, and EI a flexural stiffness.

$$F_1(\lambda) = -\lambda\,(1 - \exp(-\lambda)\,(2 \sin\lambda + \exp(-\lambda)))/f_1(\lambda)$$

$$F_2(\lambda) = -\lambda\,(\sin\lambda - \cos\lambda + \exp(-2\lambda)\,(\sin\lambda + \cos\lambda))/f_1(\lambda)$$

$$F_3(\lambda) = -\lambda^2(1 + \exp(-\lambda)\,(\exp(-\lambda) - 2\cos\lambda))/f_1(\lambda)$$

$$F_4(\lambda) = \lambda^2 \sin\lambda\,(1 - \exp(-2\lambda))/f_1(\lambda)$$

$$F_5(\lambda) = \lambda^3(1 + \exp(-\lambda)\,(2 \sin\lambda - \exp(-\lambda)))/f_1(\lambda)$$

$$F_6(\lambda) = -\lambda^3(\sin\lambda + \cos\lambda + \exp(-2\lambda)\,(\sin\lambda - \cos\lambda))/f_1(\lambda)$$

where

$$f_1(\lambda) = \cos\lambda - \exp(-\lambda)\,(2 - \exp(-\lambda)\cos\lambda).$$

Axisymmetric Vibration of Annular Plates Using Receptances

R.P. BRODZINSKI
Research Engineer, Department of Mechanical Engineering, University of Western Australia

SUMMARY A useful approach to determining the vibrational characteristics of beam systems utilizes the receptance method. However the receptance method has not been applied extensively to the analysis of plate or shell type structures. In this paper the application of receptances to the axisymmetric vibrations of annular plates is discussed. A continuous annular plate simply supported along the two boundary edges and simply supported at the intermediate support is considered. The method presented gives an exact solution and can be readily extended to any standard boundary conditions and also to non-axisymmetric vibrations.

1 INTRODUCTION

Most structures are combinations of shell, plate, beam and lumped elements. Several methods of calculating dynamic response and eigenvalues have been developed such as finite difference, transfer matrix and finite element methods. A useful approach to determining the vibrational characteristics of beam, shaft and lumped parameter systems is the receptance method discussed in detail by Bishop and Johnson, 1960. Also Sakharov, 1966 used the method of dynamic rigidities which are reciprocal receptances to calculate the vibrational characteristics of an cylindrical shell with an annular plate at one end. In a recent paper Azimi, Hamilton and Soedel, 1984 applied the receptance method to the free vibration of rectangular plates and Soedel, 1981 presented a review of the receptance method with application to shell type structures.

The object of this paper is to clarify the application of this method to the free vibration of annular plates. For the sake of simplicity only axisymmetric vibration of simply supported annular plates is considered.

2 TIP RECEPTANCES OF AN ANNULAR PLATE SIMPLY SUPPORTED ON BOTH EDGES

Consider a plate shown in Figure 1

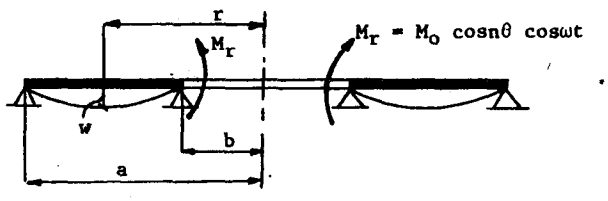


FIGURE 1 Annular plate simply supported on both edges.

The classical differential equation of motion for the transverse displacement w of a plate is given by

$$D\nabla^4 w + \rho \frac{\partial^2 w}{\partial t^2} = 0 \qquad (1)$$

where D is the flexural rigidity and is defined by

$$D = \frac{Eh^3}{12(1-\nu^2)} \qquad (2)$$

E is Young's modulus, h is the plate thickness, ν is Poisson's ratio, ρ is mass density per unit area of the plate, t is time, and $\nabla^4 = \nabla^2\nabla^2$, where ∇^2 is the Laplace operator.

When free vibrations are assumed

$$w = W \cos \omega t \qquad (3)$$

where ω is the circular frequency and W is a function only of the position coordinate r. Substituting equation (3) into equation (1) yields

$$(\nabla^4 - k^4)W = 0 \qquad (4)$$

where k is a parameter defined as

$$k^4 = \rho \frac{\omega^2}{D} \qquad (5)$$

The general solution of equation (4) is

$$W(r) = [A_n J_n(kr) + B_n Y_n(kr) + C_n I_n(kr) + F_n K_n(kr)] \cos n\theta \qquad (6)$$

where J_n and Y_n are the Bessel functions of the first and second kinds of order n, and I_n and K_n are the modified Bessel functions of the first and second kinds of order n respectively. The

constants A_n, B_n, C_n and F_n determine the mode shape and are determined from the boundary conditions.

A tip receptance for the plate of Figure 1 is derived with the aid of equation (6) and the following boundary conditions

$$\begin{aligned} w(r,t) &= 0 && \text{at } r = a \\ M_r &= 0 && \text{at } r = a \\ w(r,t) &= 0 && \text{at } r = b \\ M_r &= M_0 \cos n\theta \cos\omega t && \text{at } r = b \end{aligned} \tag{7}$$

where M_r for axisymmetric vibrations is given by

$$M_r = -D\left(\frac{\partial^2 w}{\partial r^2} + \frac{\nu}{r}\frac{\partial w}{\partial r}\right) \tag{8}$$

A tip receptance for the plate of Figure 1 is defined as

$$\alpha_{bb} = -\frac{\partial w/\partial r}{M_r} \quad \text{at} \quad r = b \tag{9}$$

If expressions (6) and (8) are introduced into the boundary conditions, the following expression for the receptance α_{bb} is obtained

$$\alpha_{bb} = \frac{1}{\Delta D}\left[\Delta_1 J_n'(\beta\lambda) + \Delta_2 Y_n'(\beta\lambda) + \Delta_3 I_n'(\beta\lambda) + \Delta_4 K_n'(\beta\lambda)\right] \tag{10}$$

where

$$\beta = \frac{b}{a}, \quad \lambda = ka$$

$$\Delta = \begin{vmatrix} J_n(\lambda) & Y_n(\lambda) & I_n(\lambda) & K_n(\lambda) \\ J_n(\beta\lambda) & Y_n(\beta\lambda) & I_n(\beta\lambda) & K_n(\beta\lambda) \\ J_n''(\beta\lambda) + \frac{\nu}{b}J_n'(\beta\lambda) & Y_n''(\beta\lambda) + \frac{\nu}{b}Y_n'(\beta\lambda) & I_n''(\beta\lambda) + \frac{\nu}{b}I_n'(\beta\lambda) & K_n''(\beta\lambda) + \frac{\nu}{b}K_n'(\beta\lambda) \\ J_n''(\lambda) + \frac{\nu}{a}J_n(\lambda) & Y_n''(\lambda) + \frac{\nu}{a}Y_n' & I_n''(\lambda) + \frac{\nu}{a}I_n'(\lambda) & K_n''(\lambda) + \frac{\nu}{a}K_n'(\lambda) \end{vmatrix}$$

$$\Delta_1 = \begin{vmatrix} Y_n(\lambda) & I_n(\lambda) & K_n(\lambda) \\ Y_n(\beta\lambda) & I_n(\beta\lambda) & K_n(\beta\lambda) \\ Y_n''(\lambda) + \frac{\nu}{a}Y_n'(\lambda) & I_n''(\lambda) + \frac{\nu}{a}I_n'(\lambda) & K_n''(\lambda) + \frac{\nu}{a}K_n'(\lambda) \end{vmatrix}$$

$$\Delta_2 = \begin{vmatrix} J_n(\lambda) & I_n(\lambda) & K_n(\lambda) \\ J_n(\beta\lambda) & I_n(\beta\lambda) & K_n(\beta\lambda) \\ J_n''(\lambda) + \frac{\nu}{a}J_n'(\lambda) & I_n''(\lambda) + \frac{\nu}{a}I_n'(\lambda) & K_n''(\lambda) + \frac{\nu}{a}K_n'(\lambda) \end{vmatrix}$$

$$\Delta_3 = \begin{vmatrix} J_n(\lambda) & Y_n(\lambda) & K_n(\lambda) \\ J_n(\beta\lambda) & Y_n(\beta\lambda) & K_n(\beta\lambda) \\ J_n''(\lambda) + \frac{\nu}{a}J_n'(\lambda) & Y_n''(\lambda) + \frac{\nu}{a}Y_n'(\lambda) & K_n''(\lambda) + \frac{\nu}{a}K_n'(\lambda) \end{vmatrix}$$

$$\Delta_4 = \begin{vmatrix} J_n(\lambda) & Y_n(\lambda) & I_n(\lambda) \\ J_n(\beta\lambda) & Y_n(\beta\lambda) & I_n(\beta\lambda) \\ J_n''(\lambda) + \frac{\nu}{a}J_n'(\lambda) & Y_n''(\lambda) + \frac{\nu}{a}Y_n'(\lambda) & I_n''(\lambda) + \frac{\nu}{a}I_n'(\lambda) \end{vmatrix} \tag{11}$$

The derivatives of the Bessel functions can be calculated using the following formulas (McLachlan, 1955)

$$\begin{aligned} 2J_n' &= J_{n-1} - J_{n+1} \\ 2Y_n' &= Y_{n-1} - Y_{n+1} \\ 2I_n' &= I_{n-1} + I_{n+1} \\ 2K_n' &= -(K_{n-1} + K_{n+1}) \end{aligned} \tag{12}$$

In a similar way the receptance α_{aa} can also be derived by appropriate change of boundary conditions i.e.

$$\begin{aligned} w(r,t) &= 0 && \text{at } r = a \\ M_r &= M_0 \cos n\theta \cos\omega t && \text{at } r = a \\ w(r,t) &= 0 && \text{at } r = b \\ M_r &= 0 && \text{at } r = b \end{aligned} \tag{13}$$

Therefore, the receptance α_{aa} is defined as

$$\alpha_{aa} = \frac{\partial w/\partial r}{M_r} \quad \text{at } r = a \tag{14}$$

Hence, the following expression for α_{aa} is obtained

$$\alpha_{aa} = -\frac{1}{\Delta D}\left[\Delta_5 J_n'(\lambda) + \Delta_6 Y_n'(\lambda) + \Delta_7 I_n'(\lambda) + \Delta_8 K_n'(\lambda)\right] \tag{15}$$

where

$$\Delta_5 = \begin{vmatrix} Y_n(\lambda) & I_n(\lambda) & K_n(\lambda) \\ Y_n(\beta\lambda) & I_n(\beta\lambda) & K_n(\beta\lambda) \\ Y_n''(\beta\lambda) + \frac{\nu}{b}Y_n'(\beta\lambda) & I_n''(\beta\lambda) + \frac{\nu}{b}I_n'(\beta\lambda) & K_n''(\beta\lambda) + \frac{\nu}{b}K_n'(\beta\lambda) \end{vmatrix}$$

$$\Delta_6 = \begin{vmatrix} J_n(\lambda) & I_n & K_n \\ J_n(\beta\lambda) & I_n(\beta\lambda) & K_n(\beta\lambda) \\ J_n''(\beta\lambda) + \frac{\nu}{b}J_n'(\beta\lambda) & I_n''(\beta\lambda) + \frac{\nu}{b}I_n'(\beta\lambda) & K_n''(\beta\lambda) + \frac{\nu}{b}K_n'(\beta\lambda) \end{vmatrix}$$

$$\Delta_7 = \begin{vmatrix} J_n(\lambda) & Y_n(\lambda) & K_n(\lambda) \\ J_n(\beta\lambda) & Y_n(\beta\lambda) & K_n(\beta\lambda) \\ J_n''(\beta\lambda) + \frac{\nu}{b}J_n'(\beta\lambda) & Y_n''(\beta\lambda) + \frac{\nu}{b}Y_n'(\beta\lambda) & K_n''(\beta\lambda) + \frac{\nu}{b}K_n'(\beta\lambda) \end{vmatrix}$$

$$\Delta_8 = \begin{vmatrix} J_n(\lambda) & Y_n(\lambda) & I_n(\lambda) \\ J_n(\beta\lambda) & Y_n(\beta\lambda) & I_n(\beta\lambda) \\ J_n''(\beta\lambda) + \frac{\nu}{b}J_n'(\beta\lambda) & Y_n''(\beta\lambda) + \frac{\nu}{b}Y_n'(\beta\lambda) & I_n''(\beta\lambda) + \frac{\nu}{b}I_n'(\beta\lambda) \end{vmatrix} \tag{16}$$

The natural frequency equation may be found from the condition that the appropriate receptance become infinite. That is, the natural frequencies of a plate under consideration are given by the equation

$$\Delta = 0 \qquad (17)$$

3 NUMERICAL EXAMPLES

In order to confirm the validity of the theory presented, the calculation of the first natural frequency has been carried out and compared with the known results in literature. Figure 2 shows the relation between frequency parameter λ and radius ratio β, for n = 0. It has been found that this curve is exactly the same as that obtained by the classical method according to Leissa, 1969.

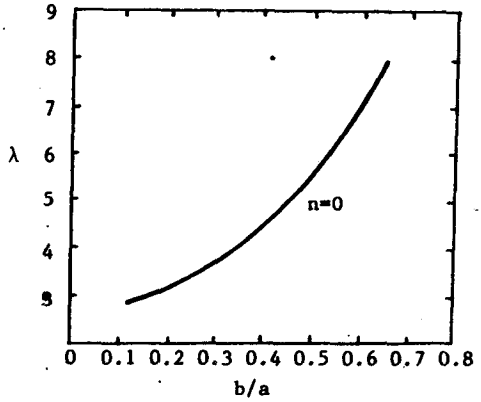


FIGURE 2 Values of λ for a simply supported, simply supported annulus, $\nu = 1/3$.

The receptances obtained allow more complex systems to be analysed. For example consider the plate shown in Figure 3.

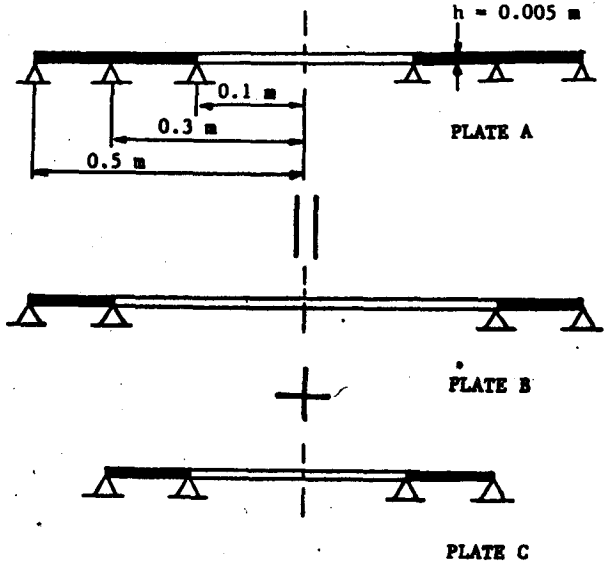
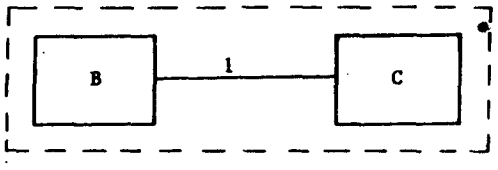


FIGURE 3 Annular plate simply supported along the boundary edges and simply supported at the intermediate support. ($E = 2.08 \times 10^{11}$ N/m^2 $\nu = 1/3$, $\rho = 39.29$ kg/m^2)

If the plate (system A) is broken into sub-systems B and C (see Figure 4), having receptances β and γ respectively, then the natural frequency equation of the plate is given by (Soedel, 1981)

$$\beta_{11} + \gamma_{11} = 0 \qquad (18)$$



SYSTEM A

FIGURE 4 Receptance model for the plate of Figure 3

The notation system for receptances adopted here is that used by Bishop, 1960 and Soedel, 1981. Therefore, index 1 means that the sub-systems are linked by co-ordinate 1 which is in this case a slope at the point where the two plates (B and C) are joined together.

The receptance β_{11} and γ_{11} are equivalent to receptances α_{bb} and α_{aa} derived in the last section. Table 1 shows some results for the plate under consideration.

TABLE I

NATURAL FREQUENCIES OF VIBRATION in rad/s for n = 0

Plate B	Plate C	Plate A
2043	1951	2062

4 CONCLUSIONS

The procedures developed in this paper based on the receptance method have proved to be adequate for the study of the vibration of annular plates. A continuous annular plate simply supported has been considered. However, the method presented can be easily extended to any standard boundary conditions and also to non-axisymmetric vibrations.

ACKNOWLEDGEMENT

The author wishes to thank Professor B.J. Stone for his interest and support given during the preparation of this paper.

5. REFERENCES

AZIMI, S., HAMILTON, J.F. and SOEDEL, W. (1984). The receptance method applied to the free vibration of continuous rectangular plates. Journal of Sound and Vibration. Vol. 93, pp. 9-29.

BISHOP, R.E.D., and JOHNSON, D.C. (1960). The Mechanics of vibration. Cambridge University Press.

LEISSA, A.W. (1969). Vibration of plates. NASA SP-160.

McLACHLAN, N.W. (1955). Bessel functions for engineers. Oxford.

需要全本请访问 www.ertongbook.com